KAWASAKI STEEL TECHNICAL REPORT
No.43 (October 2000)
Automative Materials and Instrumentation
and Process Control

Impact Energy Absorbing Capabilities and Shape Fixabilities of High Strength Steel Sheets for Automotive Bodies

Tetsuo Shimizu, Takaaki Hira, Eiji Iizuka

Synopsis :
In order to simultaneously satisfy the conflicting requirements of weight reduction and improved crashworthiness for automotive bodies, the application of high strength steel sheets is effective. For the purpose of making it possible to select material characteristics of high strength steel sheets which produce formed parts with stable shapes or to select shapes for formed parts which have suitable material characteristics for high strength steel sheets, we studied the advance evaluation of impact energy absorbing capabilities as body parts and of shape fixabilities at press forming by means of FEM simulation. As a result, we have made it clear that it is possible to evaluate the impact energy absorbing capabilities as automotive body parts taking the dynamic deformation characteristic of steel sheets into consideration. Furthermore, we have found that the material characteristic which is mainly governing the shape fixabilities changes from yielding strength to tensile strength as the bending radius decreases.

The body can be viewed from the next page.

Impact Energy Absorbing Capabilities and Shape Fixabilities of High Strength Steel Sheets for Automotive Bodies*


Tetsuo Shimizu
Senior Researcher,
Sheet Lab.,
Technical Res. Labs.


Takaaki Hira
Senior Researcher,
Sheet Lab.,
Technical Res. Labs.


Eiji Iizuka
Senior Researcher,
Sheet Lab.,
Technical Res. Labs.

Synopsis:

In order to simultaneously satisfy the conflicting requirements of weight reduction and improved crashworthiness for automotive bodies, the application of high strength steel sheets is effective. For the purpose of making it possible to select material characteristics of high strength steel sheets which produce formed parts with stable shapes or to select shapes for formed parts which have suitable material characteristics for high strength steel sheets, we studied the advance evaluation of impact energy absorbing capabilities as body parts and of shape fixabilities at press forming by means of FEM simulation. As a result, we have made it clear that it is possible to evaluate the impact energy absorbing capabilities as automotive body parts taking the dynamic deformation characteristic of steel sheets into consideration. Furthermore, we have found that the material characteristic which is mainly governing the shape fixabilities changes from yielding strength to tensile strength as the bending radius decreases.

1 Introduction

The weight of automotive bodies has been increasing in recent years due to the body parts being increasingly reinforced to increase the passenger protection due to improved and tightened crashworthiness standards. On the other hand, the requirement to reduce the body weight has been getting stronger so as to improve the fuel consumption performance and also to reduce the emission of CO_2 so as to protect the environment. By increasing the strength of steel sheets, it is possible to simultaneously improve the strength characteristics of the parts and reduce the weight through reduction of the steel sheet thickness. For this reason studies are being made to simultaneously satisfy the two opposing requirements of weight reduction and crashworthiness improvement using high strength steel sheets. With respect to the head-on crashworthiness of automobiles, for example, strength parts such as the front side members play an important role. Specifically, these members compressively deform axially and absorb impact energy at the time of a head-on collision and lighten the degree of impact on the passengers.

Conventionally, the amount of impact energy absorbed has been empirically estimated assuming that it is proportional to the product of the 0.5th power of yielding strength and the 2nd power of plate thickness.[1] However, it has become necessary to seek the optimum design of bodies which satisfies the requirements for improved crashworthiness and weight reduction at the same time and it is essential at present to correctly evaluate the impact energy absorbing characteristics of parts in advance.

Furthermore, various problems occur with the improved strength of steel sheets such as generation of wrinkles at the time of press forming, breakage of materials, spring-back of formed parts and improper shape fixation due to warp generation.

In applying high strength steel sheets to strength members, in particular, improper shape fixation is the most serious problem and some countermeasures over a wide range even including alteration of product shapes are considered necessary.[2] Therefore, if the changes in shapes at forming could be quantitatively estimated in

* Originally published in *Kawasaki Steel Giho*, **32**(2000)1, 14–20

Table 1 The Japan Iron and Steel Federation standard and hardening mechanism of typical high tensile strength steel sheets produced by Kawasaki Steel

TS grade (MPa)		JISF standard	Kawasaki Steel standard	Hardening mechanism
440	Hot rolled	JSH440W, J	SAPH440	C, Mn alloyed solid solution hardening
		JSH440B	SAPH440LC	C, Mn alloyed solid solution hardening
		JSH440R	KFR440E	C, Mn alloyed solid solution hardening
		—	SAPH440BH	C, Mn alloyed solid solution hardening and strain aging
	Cold rolled	JSC440W	APFC440	C, Si, Mn, P alloyed solid solution hardening
		JSC440P	CHR440	C, Si, Mn, P alloyed solid solution hardening
		—	CHLY440	Martensitic transformation hardening (dual phase)
	Hot-dip galvannealed	JAH440W, J	RASA440	C, Mn alloyed solid solution hardening
		JAH440R	RAAPFH440	C, Mn alloyed solid solution hardening
	Cold-dip galvannealed	JAC440W	RASAP440	C, Mn alloyed solid solution hardening
		JAC440P	RACHRX440	C, Mn, P alloyed solid solution hardening
		—	RACHLY440	Martensitic transformation hardening (dual phase)
540	Hot rolled	JSH540W	RHA540	C, Mn alloyed solid solution hardening
		JSH540B	RHA540SK	Ti-added precipiation hardened ferrite and martensitic transformation hardening
		JSH540R	RHA540F	Ti, Nb-added precipitation hardening
		JSH540Y	RHA540D	Martensitic transformation hardening (dual phase)
590	Hot rolled	JSH590W	RHA590	C, Mn alloyed solid solution hardening
		JSH590B	RHA590SK	Ti-added precipitation hardened ferrite and martensitic transformation hardening
		JSH590R	RHA590F	Ti, Nb-added precipitation hardening
		JSH590Y	RHA590D	Martensitic transformation hardening (dual phase)
		—	RHA590DX	Transformation hardening and residual austenite
		—	RHA590SH	Grain refinement hardening
	Cold rolled	JSC590R	APFC590	Low C, Ti, Nb-added precipitation hardening
		JSC590Y	CHLY590	Martensitic transformation hardening (dual phase)
		—	APFC590DX	Bainitic transformation hardening and residual austenite
	Hot-dip galvannealed	JAH590R	RAAPFC590	Low C, Ti, Nb-added precipitation hardening
	Cold-dip galvannealed	JAC590R		Low C, Ti, Nb-added precipitation hardening
		—	RACHLY590	Martensitic transformation hardening (dual phase)
780	Hot rolled	JSH780R	RHA780F	Ti, Nb-added precipitation hardening
		JSH780Y	RHA780D	Martensitic transformation hardening (dual phase)
		—	RHA780DH	Ti-added precipitation hardened ferrite and martensitic transformation hardening
		—	RHA780SH	Grain refinement hardening
	Cold rolled	JSC780Y	CHLY780	Martensitic transformation hardening (dual phase)
980	Cold rolled	JSC980Y	CHLY980	Martensitic transformation hardening (dual phase)
1 180	Cold rolled	JSC1180Y	CHLY1180	Martensitic transformation hardening (dual phase)

advance, it should become possible to considerably save the time required for designing products as well as for designing stamping dies. Furthermore, if the changes in shapes due to material characteristics of steel sheets could quantitatively be estimated, it could become possible to select material characteristics of steel sheets which are suitable for shapes of formed parts.

We are trying to solve the above problems by grasping the basic characteristics of steel sheets and by evaluating the impact energy absorbing capabilities of these sheets once formed into parts as well as the shape fixabilities at the time of press forming in advance by means of FEM simulation.

In this paper, we explain the high strength thin steel sheets for automotive strength members produced by Kawasaki Steel as well as the method of evaluating the impact energy absorbing capabilities of each kind of high strength thin steel sheets once formed into parts

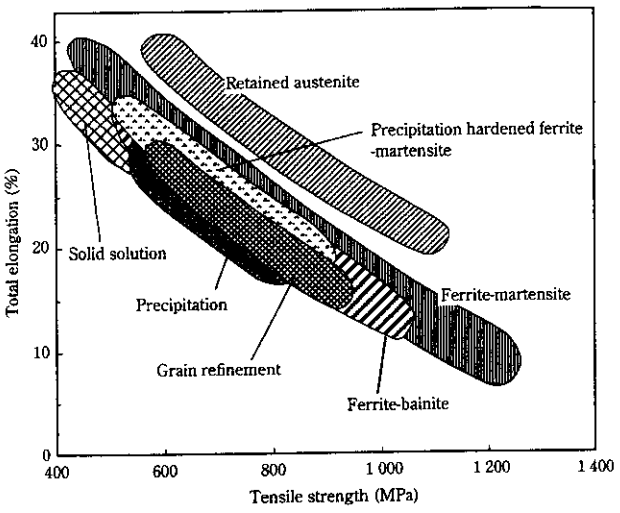

Fig. 1 Relationship between tensile strength and elongation of high strength steels

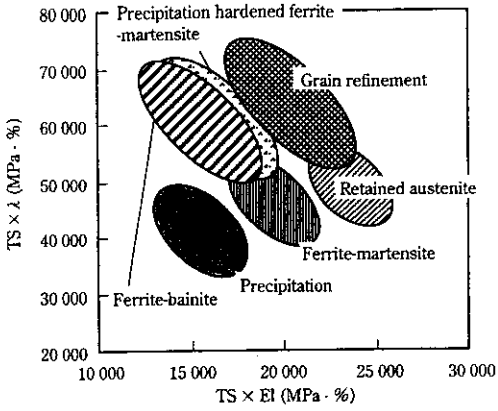

Fig. 2 Relationship between tensile strength × elongation and tensile strength × hole expanding ratio λ of 590 MPa TS grade steels

and the shape fixabilities of those steel sheets at the time of press forming.

2 Characteristics of High Strength Thin Steel Sheets for Automotive Use

As the methods to improve tensile strength of steel sheets, the following methods are generally known: (1) Solid solution hardening using various elements such as Si, Mn, and P, (2) Precipitation hardening using carbide and nitride precipitates of Ti, Nb, etc., (3) Grain refinement hardening by refining crystal grains, (4) Transformation hardening by making hard martensite and bainite phases, and (5) Dislocation hardening utilizing dislocation by means of processing.

Table 1 shows the lineup of the high tensile strength steel sheets with tensile strengths exceeding 440 MPa produced by Kawasaki Steel and the methods of hardening these steel sheets. The corresponding standards of the Japan Iron and Steel Federation are also included.

Total elongation of high strength steel during the tensile tests is an index for press formability. **Figure 1** schematically shows the relationship between the total elongation and tensile strength of high strength steel sheets for each method of hardening mentioned above. With every hardening mechanism, total elongation decreases as the tensile strength (TS) of steel sheets gets higher. However, compared with steel sheets processed by solution hardening and precipitation hardening, dual phase type high strength steel sheets produced by compounding the soft ferrite phase with the hard martensite phase show greater total elongation. Kawasaki Steel has developed hot rolled dual phase TS 590 MPa grade thin steel sheets with large total elongation[3] by applying highly accurate cooling control techniques after finishing rolling. The range of thickness of these steel sheets is 1.4–2.0 mm.

Furthermore, the company has developed steel sheets with their total elongation enhanced by making a few percent retained austenite phase appear and by using transformation induced plasticity. These steel sheets are now used for parts where bulging is the major method of forming.

The stretch flanging formability is another representative characteristic required for high strength steel sheets when being press formed and this characteristic is evaluated mainly by the hole expansion ratio λ in hole expansion tests. The relationship between tensile strength × elongation and tensile strength × hole expansion ratio λ of 590 MPa TS grade steel sheets is schematically shown in **Fig. 2**. It is known that material structures having uniform distribution of hardness are generally effective for improving the stretch flanging formability and complex structure steels with large total elongation have low stretch flanging formability because the difference in hardness between the major phase and the minor phase of these steels is large. Precipitation hardened type dual phase steels behave such that their stretch flanging formability is improved by making the difference in hardness between the major phase and the hard minor phase small. In order to obtain this result, the material is hardened by precipitation hardening TiC in the soft ferrite phase of the dual phase while maintaining the characteristic of a complex structure steel having a large total elongation. Compared with conventional steels, the precipitation hardened type dual phase steels, the TS 780 MPa grade in particular, have a higher fatigue strength, a better balance between the strength and the elongation relationship as well as a higher hole expansion ratio. This type of steel has been adopted for ultra-high strength, lightweight wheels for the first time in the world.[4]

In addition to the above, it has been considered preferable that ideal high strength materials of a high degree of forming use with superior performance both

in local elongation and uniform elongation be of a uniformly hardened structure macroscopically and of a nonuniformly hardened structure microscopically, and have many hard minor phases finely scattered to such an extent that precipitation hardening does not occur.[5] It has also been confirmed that the stretch flanging formability remarkably improves without lowering the uniform elongation by making crystal grains fine using dynamic recrystalization.[6] It is expected that the balance of elongation and stretch flanging formability will be improved by making crystal grains finer in the future.

TS440 MPa grade hot rolled steel sheets produced by making use of strain age hardening have also been developed.[7] The fatigue properties and crash performance of these steel sheets can be remarkably improved after paint baking to a level competitive with 590 MPa grade steel sheets while maintaining a formability equivalent to that of conventional 440 MPa steel sheets.

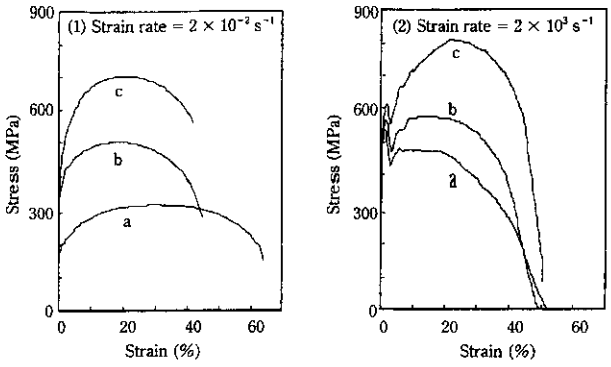

a: Mild steel
b: 440 MPa grade solid solution hardened steel
c: 590 MPa grade dual phase steel

Fig. 3 Nominal stress-nominal strain curves at strain rates of (1) $2 \times 10^{-2}\,s^{-1}$ and (2) $2 \times 10^{3}\,s^{-1}$

3 Dynamic Deformation Performance of Steel Sheets

In order to estimate the impact energy absorbing capabilities of a steel sheet as a body part in advance, it is important to accurately grasp the dynamic deformation properties of the steel sheet. We determined dynamic deformation properties of various steel sheets with different strengths by carrying out tensile tests at a strain rate of $2 \times 10^{-3}\,s^{-1}$ using an impact tensile tester applying the Hopkinson bar method.[8] The impact tensile test specimens had a width of 2.5 mm in the parallel section and a gauge length of 3.8 mm. An example of the stress-strain curves obtained is shown in **Fig. 3**. For comparison purpose, Fig. 3 also shows stress-strain curves obtained with specimens with the same strain width of the parallel section and gauge length through tensile tests at a strain rate of $2 \times 10^{-2}\,s^{-1}$ using an Instron type tensile tester.

When tested with a strain rate of $2 \times 10^{3}\,s^{-1}$, peaks were observed immediately after tensile force was applied, however, the peaks were presumably caused by vibration of the test unit and dispersion of stress waves spread over the unit or some effects of yielding phenomena. It is difficult to separate these effects from the stress-strain curves, therefore, the average of the upper and lower ends of the peak was taken as the yielding strength (YS). With every type of steel, both YS and TS increase as the strain rate gets higher and the higher the strength of steel is, the lesser the increase becomes.

We then obtained absorbed energy values caused by dynamic deformation of steel sheets of various kinds with various types of hardening mechanisms and various strengths by integrating the stress-strain curves of the higher speed tensile tests up to a strain of 30%. The relationships between the absorbed energy and the TS and YS at the lower speed tensile tests obtained are shown in **Figs. 4** and **5** respectively. With every kind of steel, absorbed energy caused by dynamic deformation increases as the TS increases. It is reported that absorbed energy increases by making the minor phase of martensite fine, thus increasing the interfacial area of the ferrite and martensite, even with the same value of TS, in the case of dual phase steel.[7] Furthermore, with dual phase steel, the absorbed energy is high despite the yield strength, as measured by low speed tensile tests, being low. This is because the initial n value of dual phase steel at dynamic deformation is higher than that of other kinds of steel.[9] As will be described later in this paper, there are some cases where spring-back at press forming becomes smaller for steel with lower YS even with the same value of TS and the dual phase steel is superior in energy absorption capability and shape fixability.

4 Estimation of Impact Energy Absorbing Capabilities of Body Parts

For the purpose of estimating impact energy absorbing capabilities of steel as an automotive body parts, we made dynamic compression deformation tests on hat shaped section similar to front side members which are typical crash resisting parts and compared the test results with that of FEM simulation.

The specimens for axial impact collapse tests were made by spot welding a 1.6 mm thick 300 mm long steel sheet which had been bent into a hat shape to a flat 1.6 mm steel sheet as shown in **Fig. 6**. The steel sheets used were of four different strengths including ultra low carbon IF mild steel, TS 440 MPa grade solid solution hardened steel, TS 590 MPa grade solid solution hardened steel and TS 590 MPa grade dual phase steel. The cross-sections of the specimens were of three sizes, i.e., large, medium and small as shown in Fig. 6. A weight of 294 N was crashed against the specimens in the axial direction at a speed of 30 km/h and 50 km/h and the dynamic deformation behaviors of these specimens were

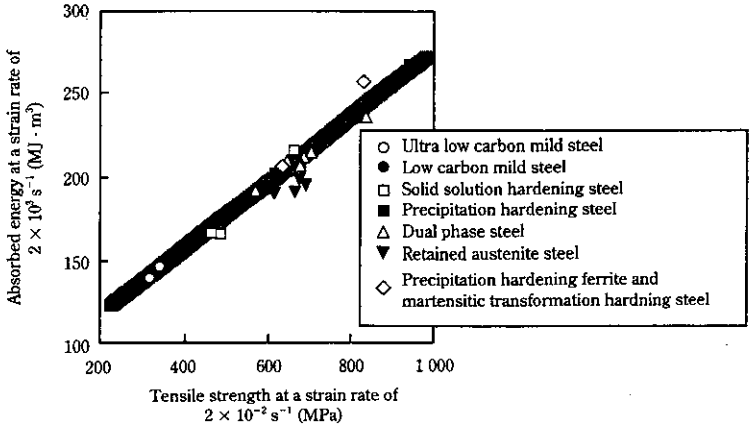

Fig. 4 Relationship between absorbed energy at a strain rate of 2×10^{-2} s^{-1} and tensile strength at a strain rate of 2×10^3 s^{-1}

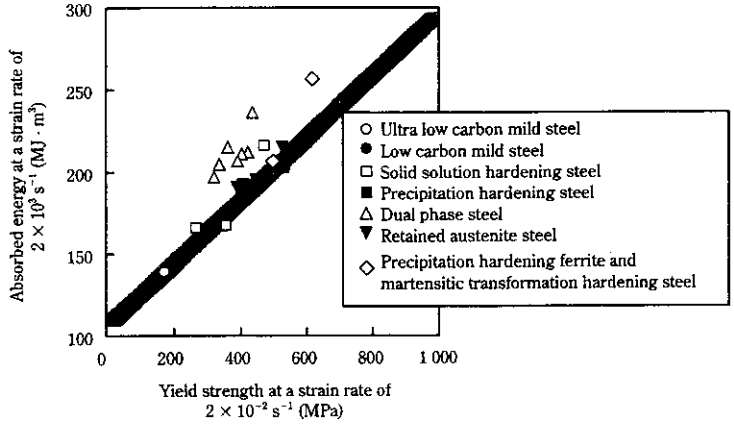

Fig. 5 Relationship between absorbed energy at a strain rate of 2×10^{-2} s^{-1} and yield strength at a strain rate of 2×10^3 s^{-1}

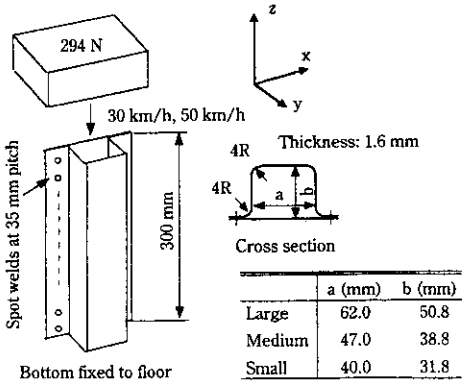

	a (mm)	b (mm)
Large	62.0	50.8
Medium	47.0	38.8
Small	40.0	31.8

Fig. 6 Schematic illustration of axial impact collapse test

analyzed.

Also LS-DYNA3D program employing the dynamic explicit solution method was used for FEM simulation. The coordinate axes were taken as shown in Fig. 6. The number of elements and nodal points per specimen were taken 1 080 and 1 096 respectively and these numbers were respectively taken 16 and 32 for the weight. The coefficient of friction between the specimen and the weight at the time of contact, that of the specimen itself at the time of contact and that between the hat shaped element and flat plate element of specimen were all taken as 0.2. As the boundary condition, displacement and rotation were totally restricted at the nodal points on the bottom surface. Displacement in the x direction and rotation around the y and z axes were restricted at the nodal points located on the opposite surface.

In order to obtain material characteristics which are to be used for FEM simulation, the methods approximated by the Cowper-Symonds formula[10] using true stress-true strain diagrams of tensile test at a low strain rate and at a high strain rate is adopted. However, when the shape of the true stress-true strain diagram at low strain rate largely differs from that at a high strain rate, the accuracy of the approximation formula decreases which is a problem. Therefore, we adopted a table system in

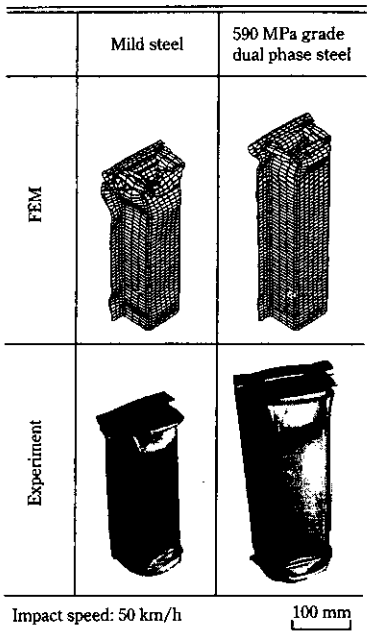

Fig. 7 FEM simulations and experimental results of axial collapse test (large cross-sectional area)

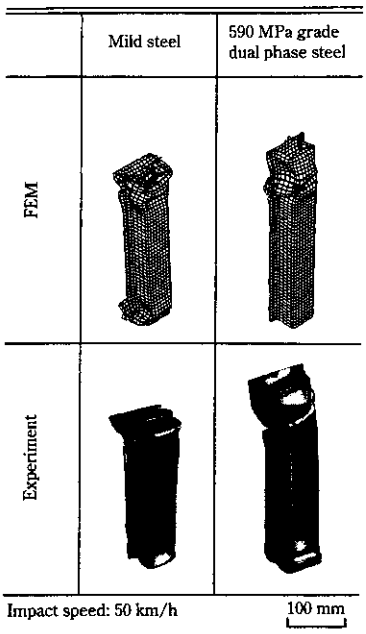

Fig. 8 FEM simulations and experimental results of axial collapse test (small cross-sectional area)

which we keep the true stress-true strain relationship at respective strain rates as values in mind and obtain the values at intermediate strain rates by interpolation.

With respect to the large specimens, examples of the specimens' shape after crashing obtained by FEM simulation and by experiment are shown in **Fig. 7**. According to the result of FEM simulation, the collapsed profiles indicated that buckling started from the end surface on the side where the weight crashed against and it was observed from deformation of the bottom member that deformation was small in the vicinity of the bottom section. Furthermore, it was observed that destruction grew severer as the strain rate increased and the specimen crushed in multistages but the higher the strength of steel was, the lower the degree of destruction became. According to the collapse tests, on the other hand, there were cases where buckling occurred from the crashed side, from the bottom section and from both and no general rule was found. This is considered to be due to the effects of the accuracy of forming the end surface, gaps in contact, etc., and suggests difficulties in the experiments. As with FEM simulation, the specimens showed multistagewise buckling when the strain rate was increased.

As for the small specimens, **Fig. 8** shows the specimens' shape after crashing obtained by FEM simulation and by experiment. Compared with the large specimens, buckling tended to occur at a location apart from the end part. With high strength steel sheet specimens crashed at a high strain rate, buckling was found to occur about 60 mm from the end point in the experiments, and also by FEM simulation. This is considered to be due to the tendency that the end part hardly collapses because the side length of the free end surface is shorter than that of large specimens.

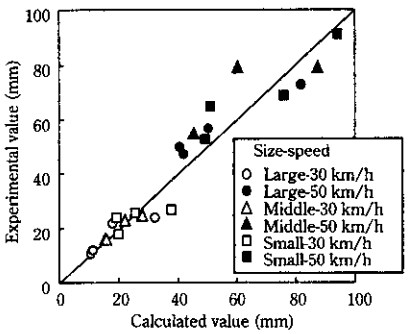

Fig. 9 Relationship between calculated values and experimental values of collapse length

Figure 9 shows a comparison of the collapse length by FEM simulation and by experiment for all cases. The two sets of values are in good agreement. It is clear that the dynamic deformation characteristics of body parts can be estimated using FEM simulation.

5 Estimation of Shape Fixabilities of High Strength Steel Sheets

Various problems occur in press forming of high strength steel sheets. It is said that, a rise in yielding points has a large effect on various shape defects of surfaces like wrinkles and surface deflectiones and on dimensional accuracy defects, and a drop of ductility

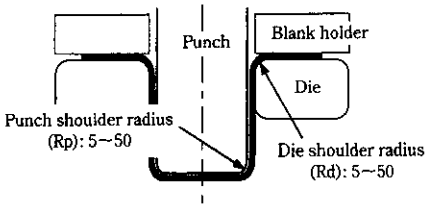

Fig. 10 Analysis model for numerical calculation

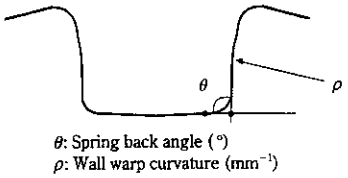

Fig. 11 Evaluation parameter of spring back behavior

(total elongation, ultimate deformation capacity) is appeared as a drop of stretch formability, stretch flanging formability and bending limit.[2)]

For use of high strength steel sheets, countermeasures against minute defects in surface shape such as surface deflection and those against defects in shape fixabilities such as spring-back and warp are important in addition to countermeasures against crack generation. For various surface shape defects in panel formation, clarification of the mechanism and quantitative evaluation have been advanced[11)] and various countermeasures such as the use of blank holder force control techniques have been developed.

On the other hand, defects in shape fixabilities are the most serious problem in applying high strength steel sheets to strength members and the mechanism of causing these defects have not been clarified. Various studies[12,13)] have been made so far on shape fixability in hat shape bend forming of high strength steel sheets and it has been known that it has some correlation with YS or TS. However, which material characteristics are governing this has not been clarified.

Therefore, by means of numerical analysis using the elasto-plastic strain increment theory[14,15)] with the anisotropy being taken into consideration, we clarified the contribution of YS and TS on shape fixabilities at hat shape bend forming.[16)]

We analyzed the shape fixability at hat shape bend forming shown in **Fig. 10**, in a shearing force neglected plane stress field on the assumption that plastic anisotropy is considered only in the direction of sheet thickness. Furthermore, we used the same method for analyzing and calculating bending, reverse bending, spring-back and warp as a method which was previously reported.[12)]

We evaluated the shape fixability after hat shape bend forming the spring-back angle θ at the punch shoulder and the warp curvature ρ of the vertical wall shown in **Fig. 11**. The materials used for analysis were of five levels including ultra low carbon IF mild steel, TS 440 MPa and TS 590 MPa grade solid solution hardened steels, TS 590 MPa grade dual-phase steel and TS 780 MPa grade precipitation hardened steel. The relationship between the equivalent plastic strain and the equivalent stress according to the Swift approximation obtained from actual stress-strain curves was used as the material characteristics. The relationship is shown in **Fig. 12**. The

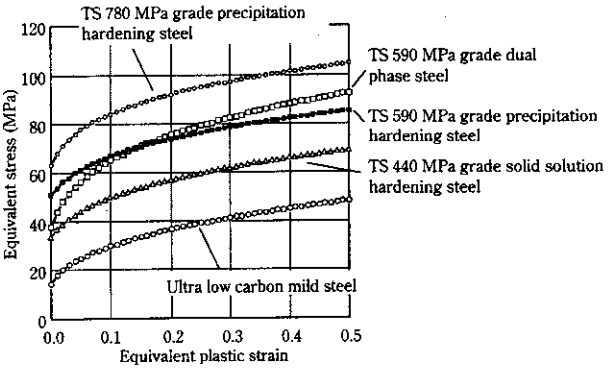

Fig. 12 Relationship between equivalent plastic strain and equivalent stress used for simulation

sheet thickness was taken as 1.6 mm in all cases. In order to investigate the effects of strength and the bending radius of steel sheets on the shape fixability, the punch shoulder radius and die shoulder radius were varied from 5 mm up to 50 mm.

An example of the effects of YS, TS and the punch shoulder radius on the spring-back angel θ is shown in **Fig. 13** (a). By comparing the correlation of the YS and TS to the spring-back angle on the basis of analysis, it was found that the correlation to the TS is higher for punch shoulder radii (Rp) smaller than 10 mm and to the YS for Rp larger than 10 mm. An example of the effects of YS, TS and die shoulder radius on the wall warp curvature ρ is shown in Fig. 13 (b). From the results of analysis, it was found that the correlation of the wall warp curvature to TS is higher for a die shoulder radii (Rd) smaller than 20 mm and that to YS is higher for Rd larger than 20 mm. On the assumption that linear relationships exist between YS and θ or ρ, and TS and θ or ρ, we evaluated these effects by the square of the correlation coefficient (the contribution rates) approximated by the least squares method. The contribution rates of YS and TS to θ are shown in **Fig. 14**. The spring-back angle θ has a stronger correlation to the YS for punch shoulder radii larger than 11 mm ($Rp/t \fallingdotseq 7$) and to the TS for radii smaller than 11 mm. The contribution rates of YS and TS to ρ are shown in **Fig. 15**. The wall warp curvature ρ has a stronger correlation with YS for those die shoulder radii larger than 22 mm ($Rd/t \fallingdotseq 7$) and with

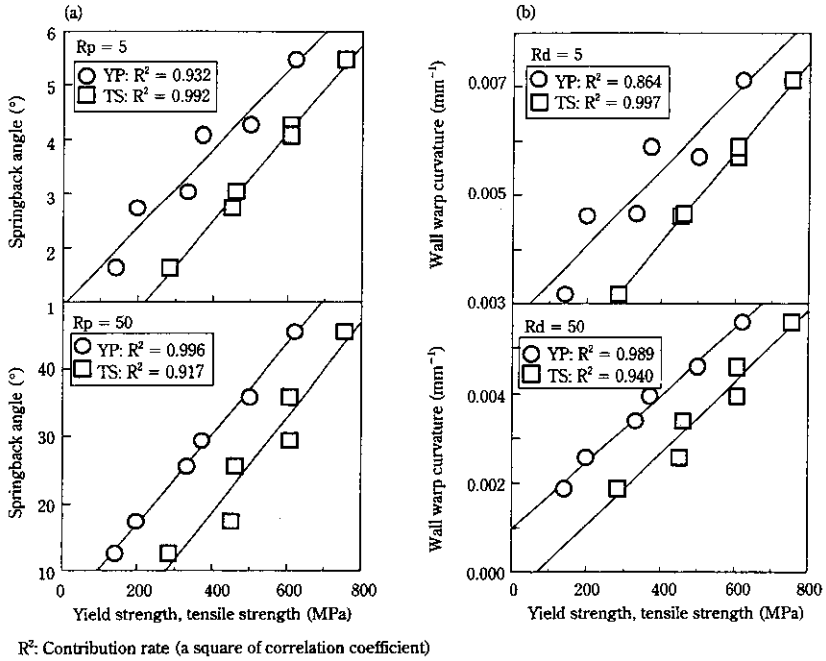

Fig. 13 Effect of yield strength and tensile strength on spring back: (a) effect of punch shoulder radius (Rp) on spring back angle, (b) effect of die shoulder radius (Rd) on wall warp curvature

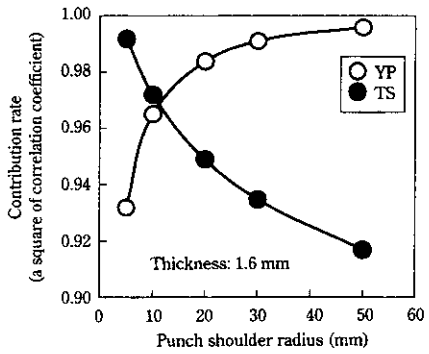

Fig. 14 Effect of punch shoulder radius on contribution rate between material strength and spring back angle

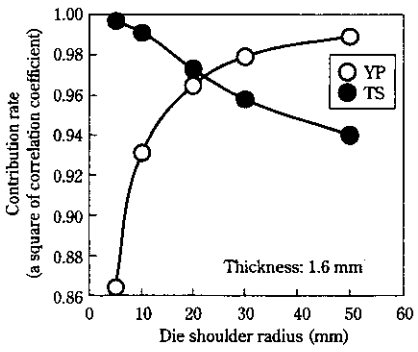

Fig. 15 Effect of die shoulder radius on contribution rate between material strength and wall warp curvature

TS for those smaller than 22 mm. In both cases, as the bending radius decreases, the correlation with the YS weakens and the correlation with the TS strengthens. This phenomenon occurs because the smaller the bending radius is, the larger plastic strain at deformation becomes, thus the bending moment becomes larger. The reason why this trend is stronger for wall warp curvature is because the strain accumulated at the die shoulder by bending deformation and unbending deformation is larger than the strain at the punch shoulder caused by bending deformation.

From the above explained results, it has become clear that the material characteristics mainly governing the shape fixabilities changes from YS to TS with a decrease of the bending radius. From this fact that shape fixabilities can be evaluated by equivalent stress at a certain level of strain. Therefore, we investigated the equivalent plastic strain at the largest equivalent stress where the analyzed correlations with θ and ρ are the largest. The results are shown in **Fig. 16**. The contribution rates of all cases were larger than 0.999. Therefore, it can be considered that shape fixabilities can be evaluated by equivalent stress at certain equivalent plastic strains. The equivalent plastic strain when evaluating shape fixabilities by equivalent stress becomes larger as the bending radius decreases and when compared with the same bending radius, the strain is larger for warps than for spring backs. With 1.6 mm steel sheets and 5 mm die

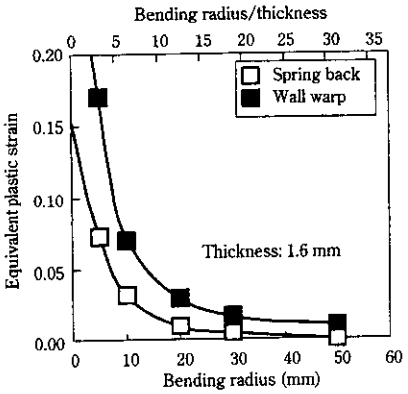

Fig. 16 Relationship between bending radius and equivalent plastic strain to evaluate shape fixability by equivalent stress

shoulder radius, for example, the wrap can be evaluated by an equivalent stress when the equivalent plastic strain is 0.17. The equivalent plastic strain when evaluating shape fixabilities by equivalent stress becomes larger as the bending radius decreases.

6 Concluding Remarks

Many years have passed since it began to be talked about that the intensive application of high strength steel sheets to structural members is important for optimizing the design of automotive bodies which simultaneously satisfy the requirements for improved crashworthiness and weight reduction. However, there still remain many obstacles which need to be overcome in the actual application of high strength steel sheets.

In order to meet the increasingly severer requirements, the development of steel sheets with excellent characteristics is necessary. At the same time, development of application techniques to automotive bodies is also important in order to fully make use of these excellent characteristics of steel sheets.

Using FEM simulation method as reported in this paper for advance evaluation of impact energy absorbing capabilities as body parts and that of shape fixabilities at the time of press forming, it becomes possible to investigate the material characteristics of steel sheets suitable for shapes of formed parts or to investigate the shapes of formed parts suitable to the material characteristics of steel sheets. Advance evaluation of such items is expected to make a large contribution first to the realization of optimum design through application of high strength steel sheets and secondly to shortening the time required for the development of automobiles as well as the time required to start production.

References

1) K. Ushioda: "Tekkou-no-Koukyoudoka-no-Saizensen", Iron and Steel Institute of Japan, (1995), 1
2) H. Hayashi: *J. of Soc. of Automotive Engineers of Jpn.*, **49** (1995)5, 11
3) T. Shimizu, N. Kanamoto, and Y. Fukui: *Kawasaki Steel Giho*, **31**(1993)3, 176
4) T. Shimizu and N. Aoyagi: *Kawasaki Steel Giho*, **31**(1999)3, 185
5) K. Kunishige: *Materia Japan*, **35**(1996)1, 32
6) E. Yasuhara, A. Tosaka, O. Furukimi, and M. Morita: *CAMP-ISIJ*, **12**(1999), 377
7) S. Kaneko, A. Tosaka, O. Furukimi, and Y. Tominaga: *Kawasaki Steel Giho*, **32**(2000)1, 67
8) N. Ao and S. Tanimura: The 2nd Materials and Proc. Conf., Jpn. Soc. of Mechanical Engineers, Tokyo, (1994), 17
9) S. Takagi, K. Miura, O. Furukimi, T. Obara, T. Kato, and S. Tanimura: *Tetsu-to-Hagané*, **83**(1997), 748
10) G. R. Cowper: Brown Univ. Div. of Applied Mech. Report No. 28, 1952
11) Ed. by Usuita-Seikei-Gijutu-Kenkyuukai: "Puresu Seikei Nanni Handbook", (1987), 85–153, [Nikkan-Kogyo-Shinnbunnsha]
12) T. Hira, E. Iizuka, and T. Kato: Society of Automotive Engineers of Japan Spring Convention, 942(1994), No. 9433245, 65
13) T. Kuwabara, N. Seki, and S. Takahashi: *Sosei-to-Kakou*, **39**(1998)453, 85
14) Y. Yamada: "Sosei-Nendansei", (1980), [Baifukan]
15) K. Misaka and K. Masui: *Sosei-to-Kakou*, **17**(1976)191, 988
16) E. Iizuka, J. Hiramoto, T. Hira, and O. Furukimi: Spring Convention, Society of Automotive Engineers of Japan, 981(1999), No. 9940305, 21